HHS Public Access

Author manuscript

J Magn Reson Imaging. Author manuscript; available in PMC 2020 December 01.

Published in final edited form as:

J Magn Reson Imaging. 2019 December ; 50(6): 1893–1904. doi:10.1002/jmri.26749.

A predictive nomogram for individualized recurrence stratification of bladder cancer using multiparametric MRI and clinical risk factors

Xiaopan Xu[1,*], **Huanjun Wang**[2,*], **Peng Du**[1], **Fan Zhang**[3], **Shurong Li**[2], **Zhongwei Zhang**[4], **Jing Yuan**[5], **Zhengrong Liang**[6], **Xi Zhang**[1], **Yan Guo**[2,#], **Yang Liu**[1,#], **Hongbing Lu**[1,#]

[1]School of Biomedical Engineering, Air Force Medical University (Fourth Military Medical University), Xi'an, Shaanxi, PR China

[2]Department of Radiology, The First Affiliated Hospital of Sun Yat-sen University, No.58 Zhongshan Second Road, Guangzhou, Guangdong, PR China

[3]Department of Radiology, The Eastern Hospital of the First Affiliated Hospital, Sun Yat-Sen University, No.183 Huangpu eastern Road, Guangzhou, Guangdong, PR China

[4]Department of Radiology, Wake Forest School of Medicine, Hanes 3055, Medical Center Boulevard, Winston Salem, NC, USA

[5]Mathematics and Statistics School, Xidian University, Xi'an, Shaanxi, PR China

[6]Departments of Radiology, School of Computer Science and Biomedical Engineering, State University of New York, Stony Brook, New York, USA

Abstract

Background—Preoperative prediction of bladder cancer (BCa) recurrence risk is critical for individualized clinical management of BCa patients.

Purpose—To develop and validate a nomogram based on radiomics and clinical predictors for personalized prediction of the first two years (TFTY) recurrence risk.

Study Type—Retrospective.

Population—Preoperative MRI datasets of 71 BCa patients (34 recurrent) were collected, and divided into training (n=50) and validation cohorts (n=21).

Field Strength/ Sequence—3.0T MRI/ T2-weighted (T2W), multi-b-value diffusion-weighted (DW) and dynamic contrast enhanced (DCE) sequences.

[#]**Corresponding authors**: i) Yan Guo, The First Affiliated Hospital of Sun Yat-sen University, No.58 Zhongshan Second Road, Guangzhou, Guangdong, 510080, PR China. dr.guoyan@163.com; ii) Yang Liu, Fourth Military Medical University, No. 169 Changle West Road, Xi'an, Shaanxi 710032, PR China. yliu@fmmu.edu.cn; iii) Hongbing Lu, Fourth Military Medical University, No. 169 Changle West Road, Xi'an, Shaanxi 710032, PR China. luhb@fmmu.edu.cn.

[*]Equal contributors.

Xiaopan Xu and Huanjun Wang contributed equally to this work, and they are co-first authors.

Declaration of Conflicting Interests

The authors of this article declare that there is no conflict of interest.

Assessment—Radiomics features were extracted from the T2W, DW, apparent diffusion coefficient and DCE images. A *Rad_Score* model was constructed by using the support vector machine-based recursive feature elimination approach and a logistic regression model. Combined with the important clinical factors, including age, gender, grade and muscle-invasive status (*MIS*) of the archived lesion, tumor size and number, surgery, and image signs like stalk and submucosal linear enhancement, a radiomics-clinical nomogram was developed. Its performance was evaluated in training and validation cohorts. The potential clinical usefulness was analyzed by the decision curve.

Statistical Tests—Univariate and multivariate analyses were performed to explore the independent predictors for BCa recurrence prediction.

Results—Of the 1872 features, the 32 with the highest area under the curve (AUC) of receiver operating characteristic were selected, and were used for the *Rad_Score* calculation. The nomogram developed by two independent predictors, *MIS* and *Rad_Score*, showed good performance in training (Accuracy 88%, AUC 0.915, $p << 0.01$) and validation cohorts (Accuracy 80.95%, AUC 0.838, $p = 0.009$). The decision curve exhibited when the risk threshold was larger than 0.3, more benefit was observed by using the radiomics-clinical nomogram than using the radiomics or clinical model alone.

Data Conclusion—The proposed radiomics-clinical nomogram has potential in the preoperative prediction of TFTY BCa recurrence.

Keywords

bladder cancer; recurrence prediction; multiparametric MRI; SVM-RFE; nomogram

Introduction

Bladder cancer (BCa) is one of the most common urological malignancies, especially for males (1–3). These tumors have a high-recurrence rate (3,4). For patients with non-muscle-invasive BCa (NMIBC), this rate could reach up to 61% during the first two years (TFTY) after transurethral resection of bladder tumor (TURBT) (3,5). Previous studies support the idea that an early radical cystectomy (RC) should be performed sooner rather than later for tumor relapse after TURBT operation to potentially increase the survival interval (6–8). Besides, for the muscle-invasive BCa (MIBC) patients, although RC with bilateral lymph nodes dissection and ileal conduit could eliminate most lesions, 5 – 50% patients would develop local or metastatic recurrences in the next 24 months (9). Preoperative prediction of the recurrence risk is, therefore, important for prognostication and individualized follow-up management of patients in TFTY after operation.

Clinically, the European Organization for the Research and Treatment of Cancer (EORTC) has proposed a risk table based on pre-treatment clinical and histo-pathological diagnoses, to individually predict the risk of recurrence and progression for patients with NMIBC, preoperatively (10). However, this predictive model only provides a qualitative stratified assessment for recurrence with Harrell's C-index of 0.597 (11,12). Developing a more precise model for preoperative individualized recurrence risk prediction is, therefore, in desirable need (12).

Previous studies have demonstrated that age at the initial surgery, gender, histological grade and muscle-invasive status (*MIS*) of the archived tumor with the maximal size in bladder lumen, tumor size, number of tumors (*NoT*), and operation choice are important factors in association with BCa recurrence (2,4,10,13). Meanwhile, through multiparametric magnetic resonance imaging (mpMRI), the low signal intensity tumor stalk observed on diffusion-weighted (DW) images has recently been confirmed useful for recurrence and progression prediction of pT1 BCa (12), and the slight submucosal linear enhancement (SLE) observed on dynamic contrast-enhanced (DCE) images is an important predictor for non-muscle invasiveness condition of BCa (14,15). Whether these image signs could be used for TFTY BCa recurrence prediction remains inconclusive up to date. In addition, preoperative radiomics strategy with nomogram models are reported to be capable of individualized recurrence risk stratification of patients with lung, hepatic and gastric cancer diseases (16–18), as well as with mental disorders like schizophrenia (19).

Based on these findings above, we hypothesized that: i) the radiomics features extracted from preoperative mpMRI to characterize the subtle variations of tissue distribution within the lesion (20–22), might be potential in predicting BCa recurrence; ii) the combination of the radiomics strategy with important clinical factors, mainly including age, gender, histological grade and *MIS* of the archived tumor with the maximal size in bladder lumen, tumor size, *NoT*, operation choice, together with the imaging signs like stalk and submucosal linear enhancement (13,23–25), might add the incremental value for TFTY BCa prediction.

Materials and methods

Patients

This retrospective study was approved by the institutional Ethics Review Board. The requirement for informed content was waived. A total of 71 patients from the ** hospital were enrolled in this study, who had been initially diagnosed with BCa followed by TURBT or RC operations between November 2011 and November 2015. The inclusion-exclusion criteria were shown in Fig. E1 of Appendix I. These patients were then successively divided into the training cohort (n=50) with an equal number of the recurrent and non-recurrent patients, who received operations before June 2014, and the validation cohort (n=21) with 9 recurrent and 12 non-recurrent patients, who received operations between June 2014 and November 2015, to make the sample groups roughly balanced in both cohorts.

Archived clinical data, such as age at the time of initial surgery, gender, histological grade, *MIS* of the archived tumor with the maximal size in bladder lumen, tumor size, *NoT*, and operation choice (TURBT or RC) were extracted from reviewing the medical records. In addition, the biomarkers like tumor stalk and *SLE*, which were reviewed independently by three radiologists with bladder MRI interpretation experience of 8 years (H.J.W.), 9 years (S.R.L.) and 32 years (Y.G.), respectively, with different opinions being resolved in consensus, were also considered as important clinical factors.

Patient follow-up and outcomes

Patients' follow-up following surgery was every 3–5 months for TFTY, every 6 months for the next two years, and annually thereafter with clinical examinations mainly including cystoscopy and imaging examinations (3,4,10,11). Radiological evaluations like CT and MRI were optionally performed by clinicians if recurrence or metastasis was suspected (3,4). The recurrent events were time to first relapse within the bladder, prostatic urethra, pelvic or the ileal neobladder regardless of TNM stage (3,4,10,11). Until the latest archived follow-ups in December 2017, 34 patients developed recurrence in TFTY. The recurrence free survival (RFS) time of each patient since the initial operation was extracted.

Image acquisition and region of interest (ROI) delineation

Before receiving the initial surgery, all patients underwent pelvic mpMRI using a 3.0T MR system (Magnetom Trio, Siemens Medical Solutions, and Erlangen, Germany) with an 8-channel phased-array pelvic coil. MpMRI including T2-weighted (T2W), DW and DCE image sequences, were performed to obtain the T2W, DW and DCE images. The corresponding apparent diffusion coefficient (ADC) maps were generated automatically from the DW images(26). Primary parameters of these sequences were described in the Appendix E1.

Before tumorous region of interest (ROI) delineation, an axial image slice of each MRI modality was selected based on obtaining the largest tumorous area of each patient. After that, a manually depicted polygonal ROI was used to segment the tumorous area on the selected images. Two radiologists (H.J.W. and S.R.L.) with bladder MRI reading experience of 8 and 9 years performed the ROI delineation with a custom-developed package independently. Then the divergence of their delineation results was carefully corrected in consensus. Considering that ADC maps were calculated from DW images by using the biexponential model with b values of 0 and 1000 s/mm^2 in this study, the tumorous ROI obtained from DW images were mapped on the ADC maps to obtain the corresponding tumorous region. Fig. 1 shows an example of the tumorous ROI delineated on T2W, DW, ADC and DCE images.

Imaging feature extraction

Preoperative radiomics features, such as the histogram features, Haralick features extracted from co-occurrence matrix (CM) (27), and features extracted from run-length matrix (RLM), neighborhood gray-tone difference matrix (NGTDM) and gray level size zone matrix (GLSZM) (27), have demonstrated their potential in recurrence risk stratification of many other cancer diseases (16–18). In this study, radiomics features, including 8 histogram features, 39 CM features, 33 RLM features, five NGTDM features (28), and 15 GLSZM features (29), were extracted from tumor ROI of each image modality to fully characterize the local, regional and global tissue distribution variations of the tumor (26,27). Detailed information about these features was shown in Table E1 of Appendix E1.

Concerning different grayscales of the original images acquired, prior to CM, RLM, NGTDM, and GLSZM features extraction, the ROI grayscales were discretized and normalized to multiple grayscales (26), including 8, 16, 32, 64, and 128 graylevel,

respectively. For each tumor ROI, 468 features including 8 histogram features, 195 CM features (39×5), 165 RLM features (33×5), 25 NGTDM features (5×5), and 75 GLSZM features (15×5) were calculated. Summing up all the features from the four MRI modalities, 1872 features (468×4) were obtained. The extraction process was performed using a publicly-shared package online available (18,26).

Feature selection and predictive performance validation

In order to verify the predictive performance of the preoperative radiomics features for TFTY BCa recurrence prediction (***hypothesis i***), first, a non-linear support vector machine (SVM)-based recursive feature elimination (SVM-RFE) approach was used to select an optimal subset of features from the training cohort for the predictive model construction (26,30). Then, its predictive performance was validated in the validation cohort.

In feature selection, the goal of SVM-RFE is to determine a ranking list for all features based on a backward sequential selection strategy (30). During each sequential iteration, the feature that has the least impact on improving the classification performance is omitted. As the algorithm continues, all the features are removed one by one, and the feature ranking list is generated based on the number of iterations when the feature was discarded (26,30). In the end, the top-ranked features are those that remained the last in the iterations. Based on the ranking list, the optimal subset which contains the first n features and obtains the highest AUC in classification, is finally determined (26,30).

Incidentally, to compare the performance of the optimal features selected by using different commonly-used feature selection approaches for BCa recurrence prediction, apart from SVM-RFE, the least absolute shrinkage and selection operator (LASSO) algorithm was also performed in the training cohort for optimal radiomics features selection (31).

The non-linear SVM classifier was employed for the prediction model construction by using the selected features and the widely-used LIBSVM package with radial basis function (RBF) (21,22). Before classification, each feature was normalized to [−1, 1]. Labels of the recurrent group were set as “+1”, and that of the non-recurrent group was set as “−1”. The grid search method was adopted in the training process to select the optimal hyperparameters for predictive model construction (21).

Performance evaluation by using both radiomics features and clinical factors

After validating the performance of the preoperative radiomics features for predicting TFTY BCa recurrence, a further investigation on whether the association of the selected radiomics features with the clinical factors could add the incremental value for TFTY BCa recurrence prediction (***hypothesis ii***), was then implemented.

First, the optimal radiomics features were put into a logistic regression model to obtain the regression coefficients (32). Then, the *Rad_Score* of each patient was calculated by using a linear combination of these selected features with their corresponding regression coefficients. Finally, the *Rad_Score* and the clinical potential factors in the training cohort were analyzed by using the univariate and multivariate regression to select the independent predictors (31,33). A nomogram was then constructed with these predictors for personalized

recurrence risk stratification (31,33). Its diagnostic performance was assessed by using the training and validation cohorts with calibration plots, area under the curve (AUC) of receiver operating characteristic (ROC) (3). The clinical benefit of this nomogram model was further verified by using the decision curve analysis (3).

Statistical analysis

All statistical analyses in this study were performed by using R statistical software (version 3.4.2., x64), and the computed *p*-values were two-sided. The univariate and multivariate regression models were performed to determine the independent predictors from clinical factors and *Rad_Score* for TFTY recurrence prediction. The Odds ratio (OR) and 95% confidence interval (CI) were calculated. AUC and Harrell's C-index were used to quantitatively evaluate the recurrence stratification and RFS estimation performance (3), and the *p*-value < 0.05 were considered significant.

Results

Clinical characteristics of the patients

The characteristics of patients in the training and validation cohorts are shown in Table 1. The median age of all the 71 patients was 65 years. Seven patients were female, and two of them were recurrent in TFTY. Tumor size of the training cohort varied in 8 ~ 64 mm, and that of the validation cohort varied in 7 ~ 56 mm. *NoT* among all patients varied in 1 ~ 4 tumors. Fifteen patients in both cohorts received radical cystectomy and 7 of them developed recurrence. Whereas, 46 patients were performed TURBT and 27 of them recurred. The median RFS for all recurrent patients was 16 months with the range of 4 ~ 23 months. Whereas the median RFS for all non-recurrent patients was 34 months with the range of 24 ~ 70 months.

Performance of the radiomics model for TFTY BC recurrence prediction

After feature selection, 32 optimal radiomics features selected by using SVM-RFE approach and 21 features selected by using LASSO approach achieved the highest AUC value in the training cohort for TFTY BCa recurrence prediction, respectively, as shown in Fig. 2. Detail descriptions of these selected features are listed in Appendix E1. Using each of the two optimal feature sets and a non-linear SVM classifier, a radiomics prediction model was developed. The performance for TFTY BCa recurrence prediction in both training and validation cohorts are shown in Table 2 and Fig. 3, which indicates that the 32 features selected by using the SVM-RFE approach have more capacity in recurrence prediction.

Among the 32 features, 19 of them were from DW image sequence, 7 from DCE image sequence, and 6 from T2W image sequence (Table E2 of Appendix E1). In addition, of these features, 19 were CM features, 7 were RLM features, four were GLSZM features, one was histogram feature, and one was NGTDM feature (Table E2 of Appendix E1),

Performance of the radiomics features in association with the clinical factors for TFTY BC recurrence prediction

With 32 optimal radiomics features selected, a *Rad_Score* formula was developed by using the logistic regression to linearly combine these features into one powerful signature, and the *Rad_Score* of each patient could be easily calculated, as shown in Appendix E1. Then, the *Rad_Score* and the important clinical risk factors were analyzed by using univariate and multivariate regression, as shown in Table 3. Of these factors, *MIS, SLE, NoT* and *Rad_Score* were significantly related to BCa recurrence ($p < 0.05$) in the univariate regression. Whereas in multivariate regression with these significant factors, *MIS* (OR 2.166, 95% CI 1.154–4.066, $p < 0.05$) and *Rad_Score* (OR 8.191, 95%CI 2.415–27.780, $p << 0.05$) were determined as the independent predictors for TFTY recurrence prediction. The radiomics-clinical nomogram model constructed by using the two independent predictors is shown in Fig. 4 (A). The calibration plots with the training and validation cohorts were depicted in Fig. 4 (B), and the decision curve analysis by using different models were illustrated in Fig. 4 (C). Based on the nomogram, if a patient with muscle-invasive BCa and the *Rad_Score* of 20, the points of the two predictors will be near 15 and 33, respectively, according to the "Points" item on the top of Fig.4 (A). Then, the "Total Points" will be 48, which corresponds to the "Recurrence Risk" of about 0.45.

Using the median recurrence risk (0.55) obtained from the patients in the training cohort, all patients were then stratified as ***high-*** or ***low-risk*** group for TFTY recurrence in both cohorts. The stratification performance was quantitatively assessed, with accuracy and AUC of 88% and 0.915 in the training cohort, and of 80.95% and 0.838 in the validation cohort, as shown in Fig. 5. Based on the stratified ***high-*** and ***low-risk*** groups in both cohorts, the Kaplan-Meier (KM) plots of RFS were depicted, as shown in Fig. 6. Its comprehensive estimation performance in the training cohort was evidently superior to that of the radiomics or clinical model, respectively, with *Harrell's C-index* of 0.897 (95% CI 0.812–0.926, $p < 0.05$), as shown in Table 4.

Discussion

The high-recurrence rate is the most critical characteristic of bladder cancer (3,4). Previous studies (3,5,9,10) have denoted that the first two years (TFTY) recurrence rate can reach up to 61% for NMIBC patients and 50% for MIBC patients after operation. Specifically, if tumor recurs after TURBT in follow-ups, an early RC is expected to increase patients' overall survival interval (6). Therefore, preoperative prediction of the recurrence risk in TFTY after operation is very crucial for individualized follow-up strategies of BCa patients.

Previous studies (14,15,25,34) have indicated that: i) postoperative DW and DCE images were capable of identifying tumor recurrence from chronic inflammation and fibrosis after TURBT or cystectomy, ii) mpMRI, including T2W, DW, ADC and DCE images, might be a complimentary and potential alternative of cystoscopy for post-treatment follow-up and recurrence surveillance. Whether the preoperative mpMRI with the radiomics strategy are capable of predicting BCa recurrence, remains unknown up to now.

This study is the first to explore and validate the radiomics-clinical nomogram model based on high-throughput radiomics features extracted from preoperative mpMRI, together with the important clinical risk factors, for individualized TFTY BCa recurrence risk stratificatio after operation, preoperatively.

In extraction of radiomics feature, owing to different original grayscales of the mpMRI, grayscale normalization is indispensable, prior to the second order and high order features calculation. Hence, a multi-grayscale normalization strategy with five commonly-normalized grayscales was performed (26), from which many more features potentially useful for recurrence prediction might be extracted. With 32 features selected by using the SVM-RFE approach, the discriminative performance both in the training and validation cohorts was evaluated with a non-linear SVM, suggesting a promising effect for preoperative BCa recurrence prediction. In addition, these results were obviously better than that of the 21 features selected by using the widely-applied LASSO approach.

Of these optimal features selected, the majority of them were from DW image sequence, indicating that preoperative DW image sequence might have a preferable effect in predicting tumor recurrence. In addition, when taking a look at the feature categories, most of these selected features were CM and RLM features, preliminarily denoting that these features might well characterize the tissue heterogeneity and histo-pathologic property differences among BCa patients (35–37), thus play a key role in TFTY BCa recurrence stratification. The CM features predominately describe the gray-level distribution patterns of the neighboring pixel pairs, reflecting the local heterogeneity variations of different tumor tissues. A gray-level run is a set of consecutive, collinear pixels share the same or roughly similar gray-levels within the image, and the length of the run indicates the number of pixels in each run (38). Therefore, the RLM features are designed to characterize the distribution patterns of the gray-level run length within the tumor tissue, thus well reflect the regional heterogeneity differences of tumor tissues.

Recent studies (3,4,10,13,39) have denoted that *age*, *gender*, *grade*, *MIS/TNM stage*, *tumor size*, *NoT*, and *operation* are in association with BCa recurrence. Besides, *Stalk* and *SLE* were important image markers useful for BCa staging and muscle invasiveness discrimination (2,23,24,40). Whether these two factors are significantly related to TFTY BCa recurrenceprediction remains inconclusive to date. The results of univariate and multivariate analyses suggest that i) *MIS*, *SLE*, *NoT* and *Rad_Score* are significantly in association with TFTY BCa recurrence; ii) *MIS* and *Rad_Score* are independent predictors for TFTY BCa recurrence prediction.

Using *MIS* and *Rad_Score*, the radiomics-clinical nomogram was developed with the training cohort for recurrence risk stratification. The AUC of the nomogram model was significantly higher than that of the radiomics model, suggesting an incremental value of integrating the radiomics features with clinical predictors for BCa recurrence prediction. The calibration plots further demonstrate the effectiveness of t prediction performance. The decision curve analyses clearly suggest that the radiomics-clinical nomogram model could obtain better net benefit than the clinical model or the radiomics model when the risk threshold was larger than 0.3.

In addition, by using the KM plot analyses, the performance of the radiomics-clinical nomogram was demonstrated significantly useful for the estimation of RFS in this study. Compared with the long-term outcome overall survival, RFS is an end point that avoids extended follow-up and enables earlier adjustment of therapy. Thus, this study may present a more efficient tool that enables earlier personalized decision-making for the management of patients with BCa.

However, the results of this study should be carefully interpreted due to several actual limitations. Above all, inherent bias might exist because of the retrospective nature of this current study with limited patient cohort from a single institution. A larger database from multiple centers is in further need to external verify the overall performance of the proposed approach. What's more, other potentially useful predictors (3,4), such as tumor locations, pretreatment urine cytology, pre-recurrent times are not included in the current study because of the incomplete archived database, which would be further analyzed in multi-clinical investigation. In addition, the key genomic biomarkers (13) reported to be closely related to BCa recurrence should also be added in the nomogram to improve its overall performance. Additionally, considering that the lymph nodal (LN) involvement is an important predictor of prognosis, and patients with LN metastasis usually have a poor prognosis, one of the future works is to investigate whether the combination of T2W, DW and DCE radiomics features could add incremental value for LN status prediction.

In conclusion, as the first attempt to address the critical clinical issue, our results preliminarily demonstrate that preoperative radiomics features extracted from mpMRI, together with the important clinical risk factors, have potential in the preoperative prediction of TFTY BCa recurrence.

Supplementary Material

Refer to Web version on PubMed Central for supplementary material.

Acknowledgement

This work was partially supported by the National Natural Science Foundation of China under grant No.81871424, No.81701747 and No.81421003, National Key Research and Development Program of China under grant No. 2017YFC0107400, NIH/NCI grant #CA206171, Key project supported by Military Science and Technology Foundation under grant No.BWS14C030 and Natural Science Foundation of Guangdong Province under grant No. 2017A030313902.

References

1. Siegel RL, Miller KD, Jemal A. Cancer statistics, 2018. CA Cancer J Clin 2018;68(1):7–30. [PubMed: 29313949]
2. Babjuk M, Bohle A, Burger M, et al. EAU Guidelines on Non-Muscle-invasive Urothelial Carcinoma of the Bladder: Update 2016. Eur Urol 2017;71(3):447–461. [PubMed: 27324428]
3. Soukup V, Capoun O, Cohen D, et al. Risk Stratification Tools and Prognostic Models in Non-muscle-invasive Bladder Cancer: A Critical Assessment from the European Association of Urology Non-muscle-invasive Bladder Cancer Guidelines Panel. European urology focus 2018.
4. Kim HS, Jeong CW, Kwak C, Kim HH, Ku JH. Novel nomograms to predict recurrence and progression in primary non-muscle-invasive bladder cancer: validation of predictive efficacy in

comparison with European Organization of Research and Treatment of Cancer scoring system. World journal of urology 2018.

5. Sylvester R, Meijden A, Oosterlinck W, et al. Predicting recurrence and progression in individual patients with stage Ta T1 bladder cancer using EORTC risk tables: a combined analysis of 2596 patients from seven EORTC trials. Eur Urol 2006;49(3):466–475. [PubMed: 16442208]
6. van Rhijn BW, Burger M, Lotan Y, et al. Recurrence and progression of disease in non-muscle-invasive bladder cancer: from epidemiology to treatment strategy. Eur Urol 2009;56(3):430–442. [PubMed: 19576682]
7. Kobayashi T, Owczarek TB, McKiernan JM, Abate-Shen C. Modelling bladder cancer in mice: opportunities and challenges. Nature reviews Cancer 2015;15(1):42–54. [PubMed: 25533675]
8. Sanli O, Dobruch J, Knowles MA, et al. Bladder cancer. Nature reviews Disease primers 2017;3:17022.
9. Alfred Witjes J, Lebret T, Comperat EM, et al. Updated 2016 EAU Guidelines on Muscle-invasive and Metastatic Bladder Cancer. Eur Urol 2017;71(3):462–475. [PubMed: 27375033]
10. Cambier S, Sylvester RJ, Collette L, et al. EORTC Nomograms and Risk Groups for Predicting Recurrence, Progression, and Disease-specific and Overall Survival in Non-Muscle-invasive Stage Ta-T1 Urothelial Bladder Cancer Patients Treated with 1–3 Years of Maintenance Bacillus Calmette-Guerin. Eur Urol 2016;69(1):60–69. [PubMed: 26210894]
11. Xylinas E, Kent M, Kluth L, et al. Accuracy of the EORTC risk tables and of the CUETO scoring model to predict outcomes in non-muscle-invasive urothelial carcinoma of the bladder. British journal of cancer 2013;109(6):1460–1466. [PubMed: 23982601]
12. Yajima S, Yoshida S, Takahara T, et al. Usefulness of the inchworm sign on DWI for predicting pT1 bladder cancer progression. European radiology 2019.
13. Mari A, Campi R, Tellini R, et al. Patterns and predictors of recurrence after open radical cystectomy for bladder cancer: a comprehensive review of the literature. World journal of urology 2018;36(2):157–170. [PubMed: 29147759]
14. Wang H, Pui M, Guo Y, Yang D, Pan B, Zhou X. Diffusion-weighted MRI in bladder carcinoma: the differentiation between tumor recurrence and benign changes after resection. Abdominal imaging 2014;39(1):135–141. [PubMed: 24072383]
15. Wang H, Pui MH, Guan J, et al. Comparison of Early Submucosal Enhancement and Tumor Stalk in Staging Bladder Urothelial Carcinoma. AJR-American Journal of Roentgenology 2016;207(4): 797–803. [PubMed: 27505309]
16. Shen C, Liu Z, Guan M, et al. 2D and 3D CT Radiomics Features Prognostic Performance Comparison in Non-Small Cell Lung Cancer. Translational oncology 2017;10(6):886–894. [PubMed: 28930698]
17. Zheng BH, Liu LZ, Zhang ZZ, et al. Radiomics score: a potential prognostic imaging feature for postoperative survival of solitary HCC patients. BMC cancer 2018;18(1):1148. [PubMed: 30463529]
18. Jiang Y, Yuan Q, Lv W, et al. Radiomic signature of (18)F fluorodeoxyglucose PET/CT for prediction of gastric cancer survival and chemotherapeutic benefits. Theranostics 2018;8(21): 5915–5928. [PubMed: 30613271]
19. Cui L-B, Liu L, Wang H-N, et al. Disease Definition for Schizophrenia by Functional Connectivity Using Radiomics Strategy. Schizophrenia Bulletin 2018;44(5):1053–1059. [PubMed: 29471434]
20. Xu X, Liu Y, Zhang X, et al. Preoperative prediction of muscular invasiveness of bladder cancer with radiomic features on conventional MRI and its high-order derivative maps. Abdominal radiology 2017;42(7):1896–1905. [PubMed: 28217825]
21. Xu X, Zhang X, Tian Q, et al. Three-dimensional texture features from intensity and high-order derivative maps for the discrimination between bladder tumors and wall tissues via MRI. International journal of computer assisted radiology and surgery 2017;12(4):645–656. [PubMed: 28110476]
22. Zhang X, Xu X, Tian Q, et al. Radiomics assessment of bladder cancer grade using texture features from diffusion-weighted imaging. Journal of magnetic resonance imaging : JMRI 2017;46(5): 1281–1288. [PubMed: 28199039]

23. Wang HJ, Pui MH, Guan J, et al. Comparison of Early Submucosal Enhancement and Tumor Stalk in Staging Bladder Urothelial Carcinoma. American Journal of Roentgenology 2016;207(4):797–803. [PubMed: 27505309]
24. Takeuchi M, Sasaki S, Ito M, et al. Urinary Bladder Cancer: Diffusionweighted MR Imaging—Accuracy for Diagnosing T Stage and Estimating Histologic Grade1. Radiology 2009;251(1):112–121. [PubMed: 19332849]
25. Panebianco V, Narumi Y, Altun E, et al. Multiparametric Magnetic Resonance Imaging for Bladder Cancer: Development of VI-RADS (Vesical Imaging-Reporting And Data System). Eur Urol 2018;74(3):294–306. [PubMed: 29755006]
26. Xu X, Zhang X, Tian Q, et al. Quantitative Identification of Nonmuscle-Invasive and Muscle-Invasive Bladder Carcinomas: A Multiparametric MRI Radiomics Analysis. Journal of magnetic resonance imaging : JMRI 2018;10.1002/jmri.26327.
27. Lambin P, Leijenaar RTH, Deist TM, et al. Radiomics: the bridge between medical imaging and personalized medicine. Nature reviews Clinical oncology 2017;14(12):749–762.
28. Amadasun M, King R. Texural Features Corresponding to Texural Properties. IEEE Transactions on Systems, Man, and Cybernetics 1989;19(5):1264–1274.
29. Thibault G, Angulo J, Meyer F. Advanced statistical matrices for texture characterization: application to cell classification. IEEE Transactions on Biomedical Engineering 2014;61(3):630–637. [PubMed: 24108747]
30. Fehr D, Veeraraghavan H, Wibmer A, et al. Automatic classification of prostate cancer Gleason scores from multiparametric magnetic resonance images. PNAS 2015;112(46):E6265–6273. [PubMed: 26578786]
31. Huang YQ, Liang CH, He L, et al. Development and Validation of a Radiomics Nomogram for Preoperative Prediction of Lymph Node Metastasis in Colorectal Cancer. Journal of clinical oncology : official journal of the American Society of Clinical Oncology 2016;34(18):2157–2164. [PubMed: 27138577]
32. Li Z, Li H, Wang S, et al. MR-Based Radiomics Nomogram of Cervical Cancer in Prediction of the Lymph-Vascular Space Invasion preoperatively. Journal of magnetic resonance imaging : JMRI 2018.
33. Wu S, Zheng J, Li Y, et al. A Radiomics Nomogram for the Preoperative Prediction of Lymph Node Metastasis in Bladder Cancer. Clinical Cancer Research 2017;23(22):6904–6911. [PubMed: 28874414]
34. Thoeny HC, Bellin MF, Comperat EM, Thalmann GN. Vesical Imaging-Reporting and Data System (VI-RADS): Added Value for Management of Bladder Cancer Patients? Eur Urol 2018.
35. Lerski RA, Straughan K, Schad LR, Boyce D, Blüml S, Zuna I. MR image texture analysis—An approach to tissue characterization. Magnetic Resonance Imaging 1993;11(6):873–887. [PubMed: 8371643]
36. Fetit AE, Jan N, Peet AC, Arvanitits TN. Three-dimensional textural features of conventional MRI improve diagnostic classification of childhood brain tumours. NMR in biomedicine 2015;28(9):1174–1184. [PubMed: 26256809]
37. Liu Y, Xu X, Yin L, Zhang X, Li L, Lu H. Relationship between Glioblastoma Heterogeneity and Survival Time: An MR Imaging Texture Analysis. American Journal of Neuroradiology 2017;38(9):1695–1701. [PubMed: 28663266]
38. Galloway MM. Texture Analysis Using Gray Level Run Lengths. Computer Graphics and Image Processing 1975; 4:172–179
39. Shariat SF, Palapattu GS, Karakiewicz PI, et al. Discrepancy between clinical and pathologic stage: impact on prognosis after radical cystectomy. Eur Urol 2007;51(1):137–149; discussion 149–151. [PubMed: 16793197]
40. Babjuk M, Burger M, Zigeuner R, et al. EAU guidelines on non-muscle-invasive urothelial carcinoma of the bladder: update 2013. Eur Urol 2013;64(4):639–653. [PubMed: 23827737]

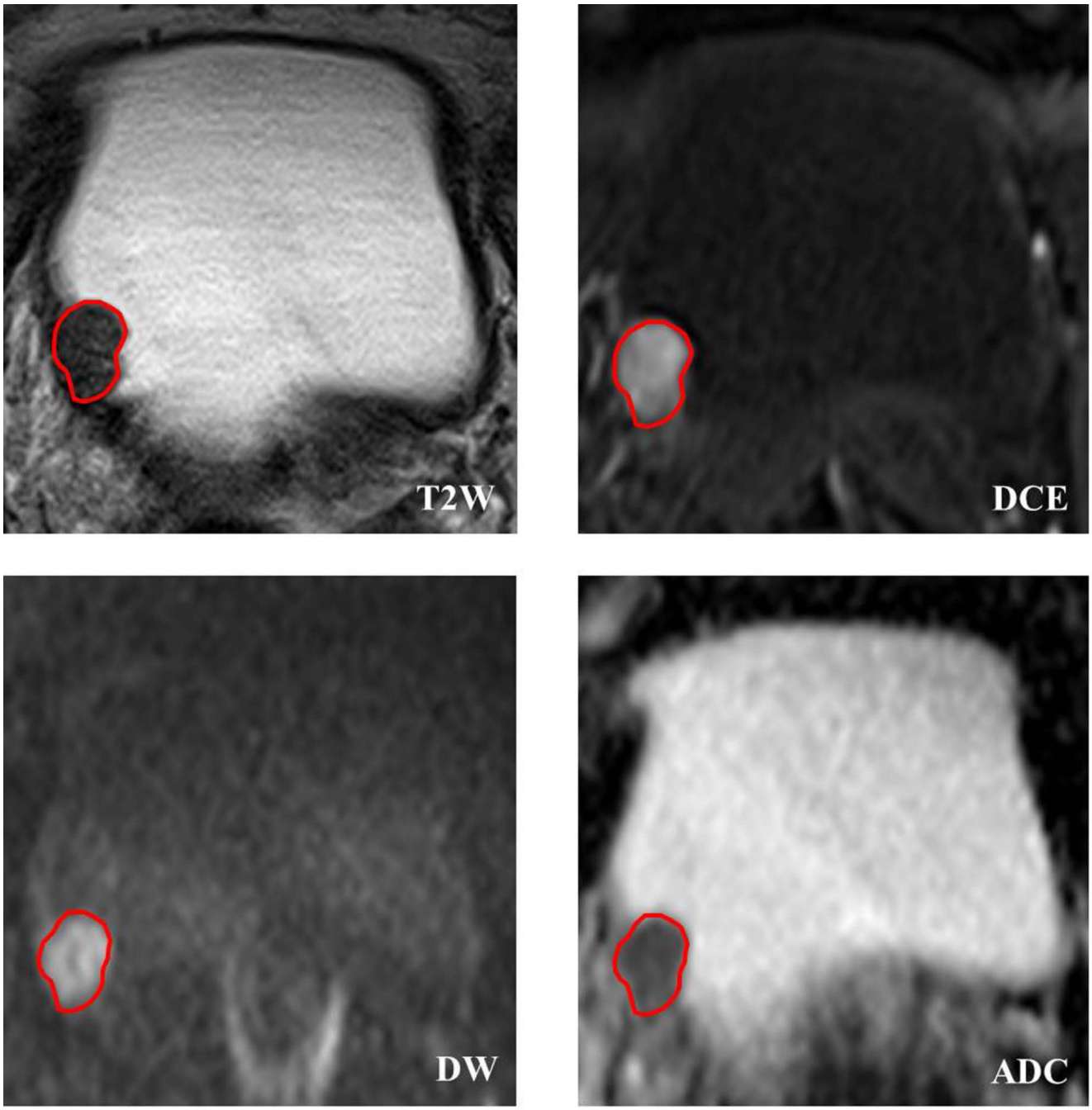

Figure 1.

Bladder tumor ROI delineated on mpMRI, including T2W, DCE, DW and ADC images. Owing to the ADC maps were derived from DW images by using the biexponential model with b values of 0 and 1000 s/mm^2, the ROI delineated on DW images can be straightforwardly mapped on ADC maps for tumor segmentation.

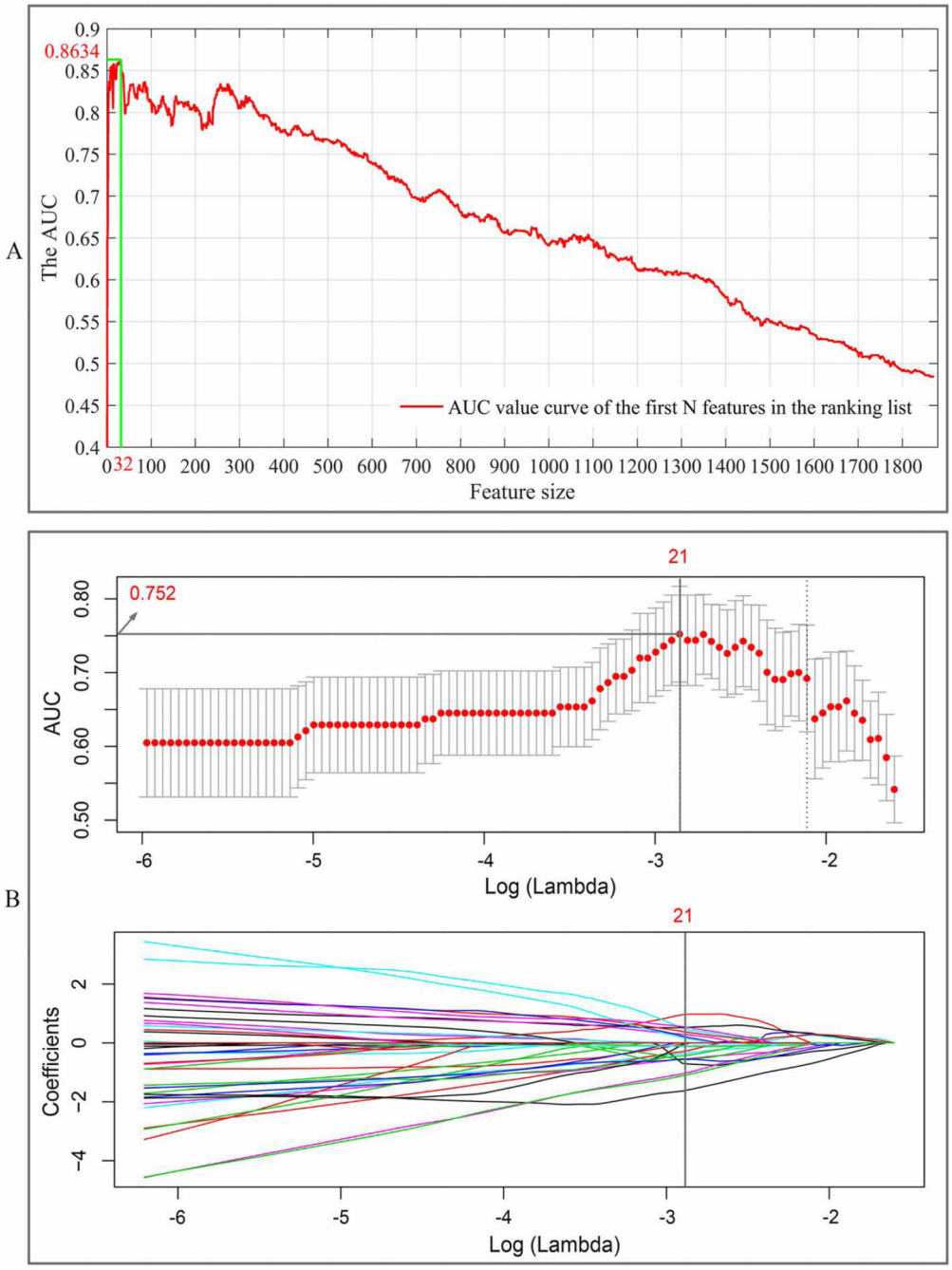

Figure 2.

Features selection process: (A) using SVM-RFE with the training cohort, 32 optimal features with the best discriminative capability were selected for the-first-two-year recurrence prediction; (B) using LASSO regression algorithm, 21 optimal features with the best discriminative capability were selected. The top sub-image of (B) depicts the tuning parameters (λ) in the LASSO model via 5-fold CV based on minimum criteria, and the bottom sub-image of (B) shows the LASSO coefficient profiles of the 1872 radiomics features. The solid vertical line was plotted at optimal tuning parameters (λ) selected.

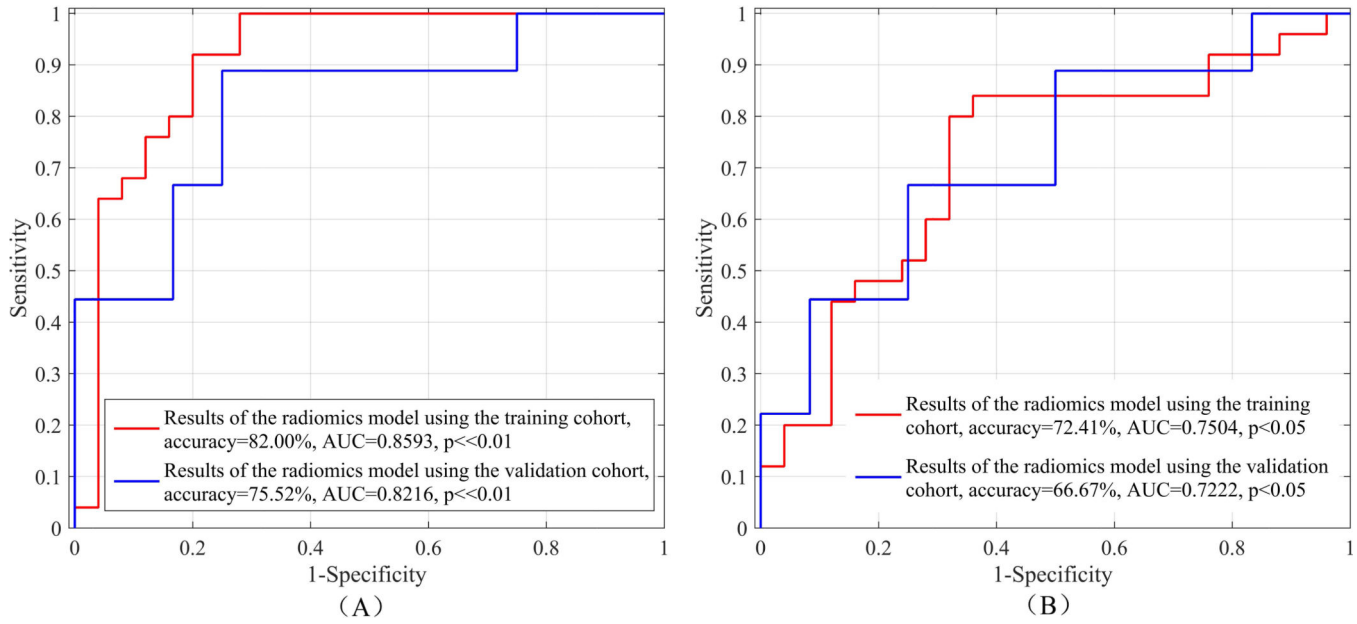

Figure 3:

Results of the optimal radiomics features selected by using SVM-RFE (A) and LASSO (B) with a non-linear SVM classifier, respectively, for TFTY BCa recurrence prediction in the training and validation cohorts.

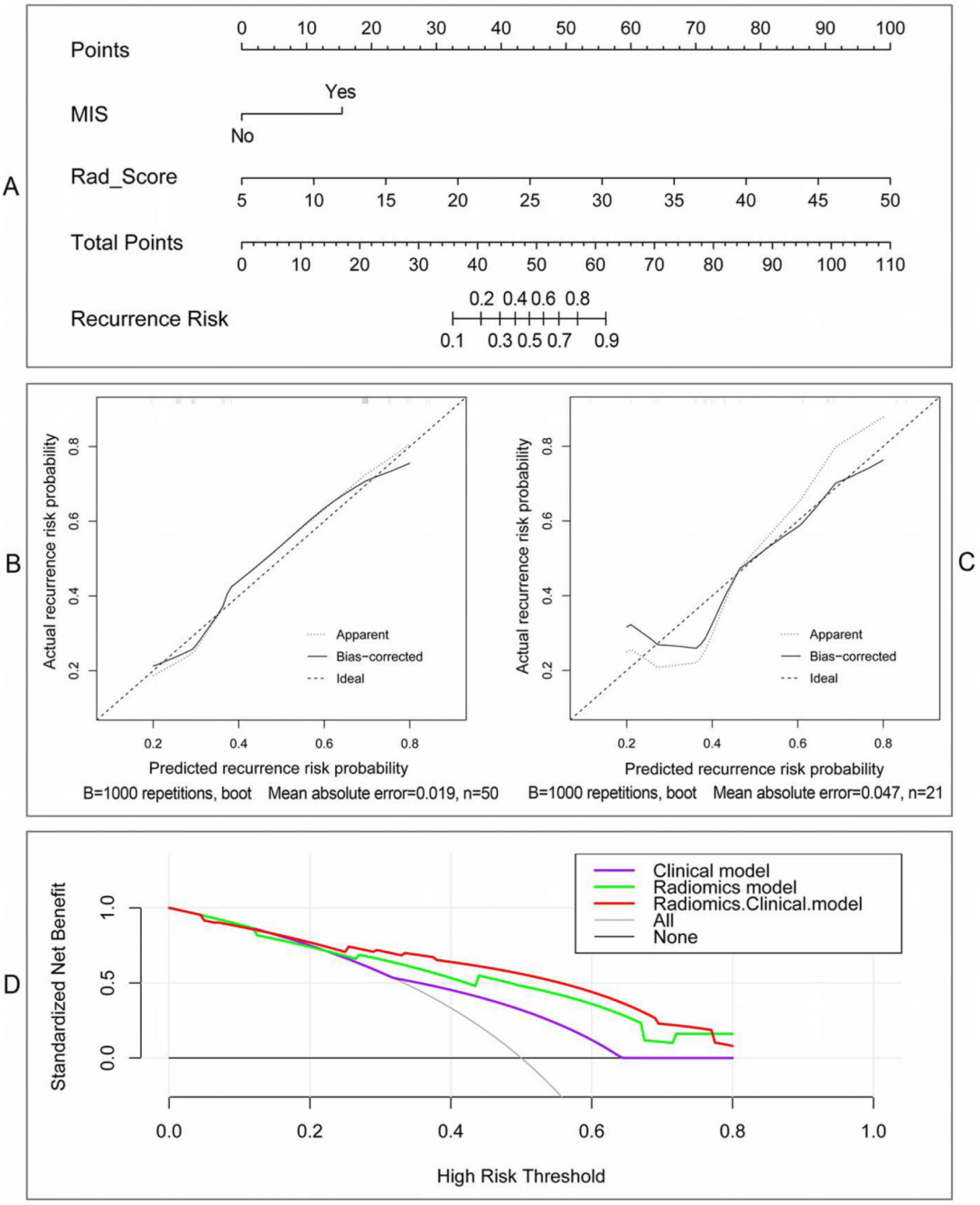

Figure 4.

Nomogram and its diagnostic performance by using the independent indicators: (A) The nomogram constructed with patient *MIS* and *Rad_Score*; (B) and (C) are calibration curves of the nomogram model with training and validation cohorts, respectively; (D) Decision curve analyses indicate the net benefit increment for the-first-two-year recurrence risk prediction by using the radiomics & clinical model compared with the radiomics model or the clinical model.

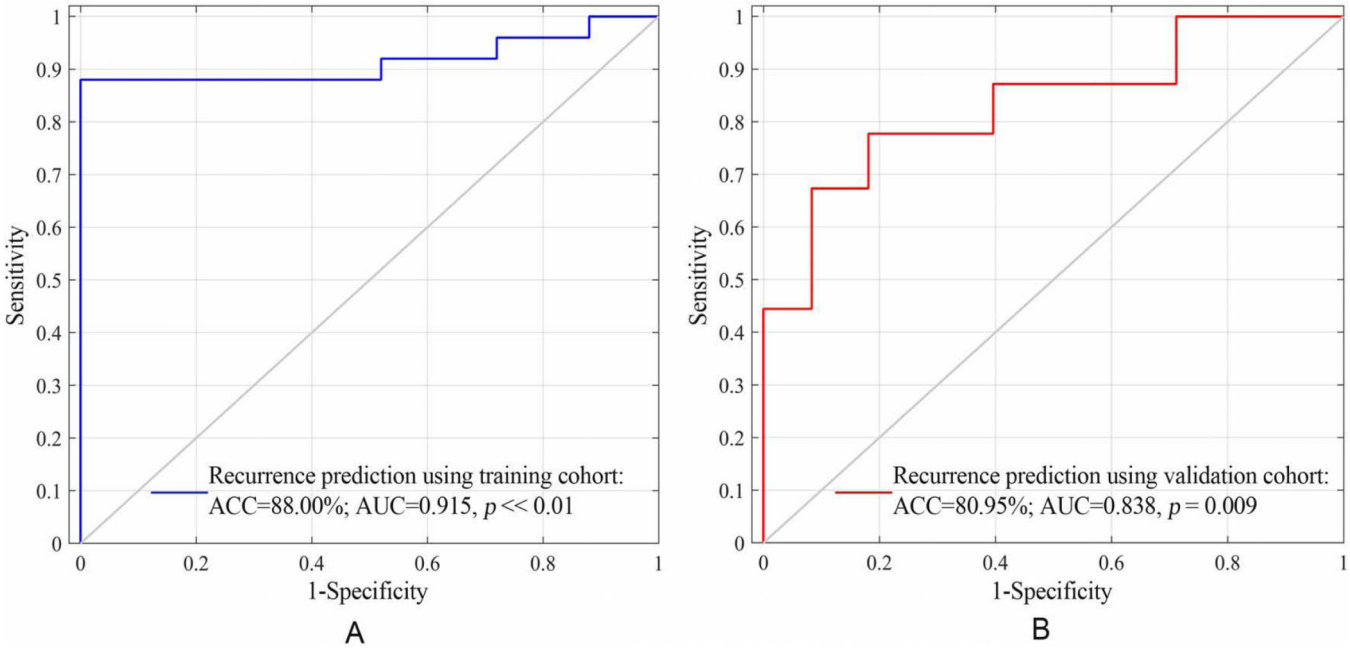

Figure 5:

ROC curves of using the radiomics_clinical nomogram model for the-first-two-year recurrence risk stratification in the training and validation cohorts

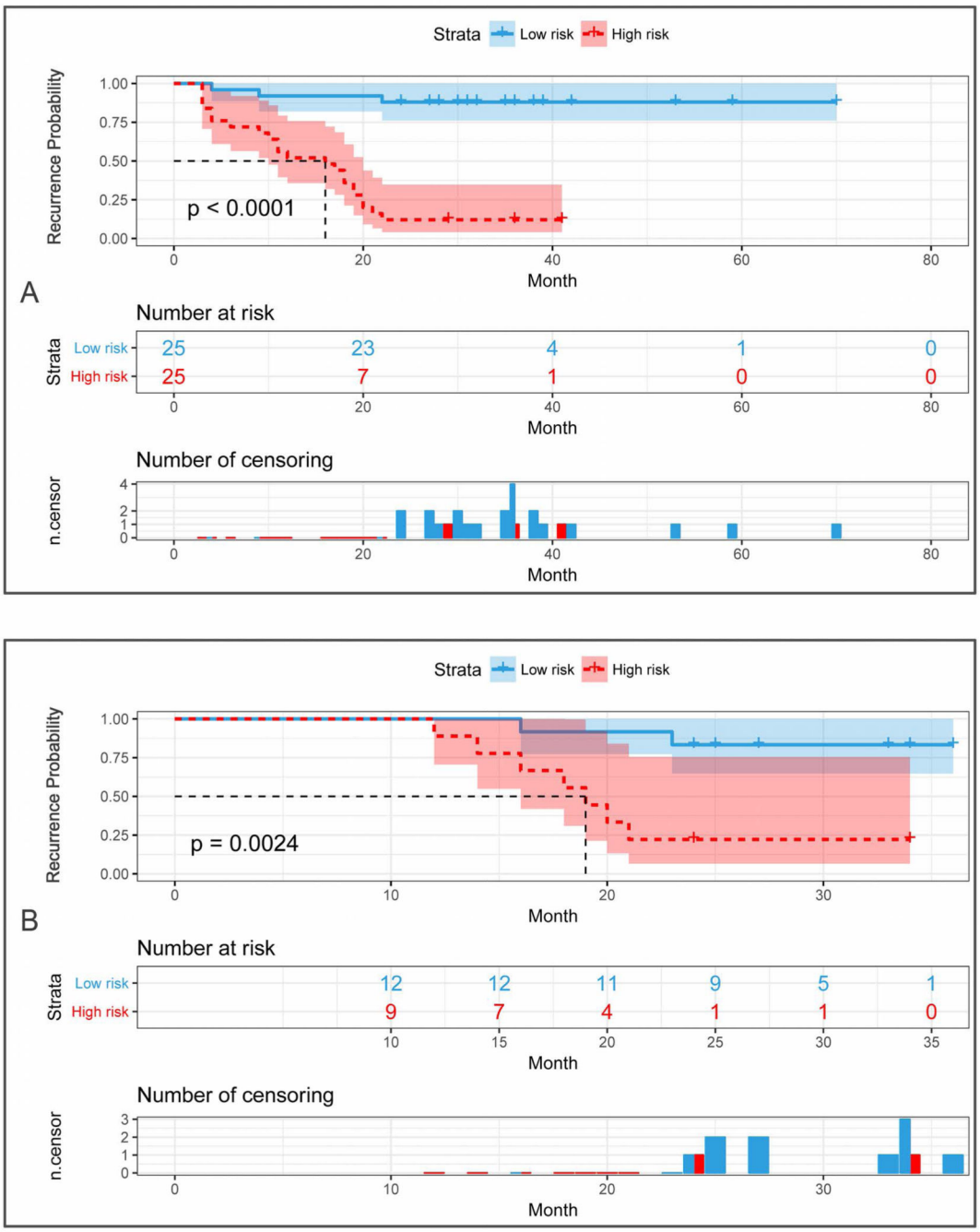

Figure 6:

Kaplan-Meier plots of the-first-two-year RFS in the training (A) and validation cohorts (B) according to the nomogram-based recurrence risk stratification

Table 1:

Demographics and clinical characteristics of patients in the training and validation cohorts

Characteristics	Training cohort (n=50)		Validation cohort (n=21)	
	Recurrent (n=25, 50%)	Non-recurrent (n=25, 50%)	Recurrent (n=9, 42.86%)	Non-recurrent (n=12, 57.14%)
Age, median (range), yrs	67 (46, 85)	64 (36, 80)	68 (51, 87)	64 (38, 79)
> 65 yrs, No. (%)	14 (28%)	11 (22%)	7 (33.33%)	4 (19.05%)
⩽ 65 yrs, No. (%)	11 (22%)	14 (28%)	2 (9.53%)	8 (38.10%)
Gender, No. (%)				
Female	2 (4%)	3 (6%)	0 (0%)	2 (9.52%)
Male	23 (46%)	22 (44%)	9 (42.86%)	10 (47.62%)
Grade				
Low	8 (16%)	9 (18%)	4 (19.05%)	5 (23.81%)
High	17 (34%)	16 (32%)	5 (23.81%)	7 (33.33%)
*MIS				
NMIBC (Stage⩽T1)	7 (14%)	15 (30.00%)	6 (28.57%)	8 (38.10%)
MIBC (Stage⩾T2)	18 (36%)	10 (20.00%)	3 (14.29%)	4 (19.05%)
Stalk				
Without	20 (40%)	12 (24%)	6 (28.57%)	8 (38.10%)
With	5 (10%)	13 (26%)	3 (14.29%)	4 (19.05%)
*SLE				
Without	17 (34.00%)	11 (22%)	7 (33.33%)	5 (36.36%)
With	8 (16.00%)	14 (28%)	2 (9.53%)	7 (33.33%)
*TumorSize, median(range), mm	25 (8, 53)	26 (12, 64)	17 (7, 26)	33 (11, 56)
*_NoT_, median (range)	1 (1, 4)	1 (1, 2)	1 (1, 4)	1 (1, 2)
Operation				
TURBT	20 (40%)	19 (38%)	7 (33.33%)	10 (47.62%)
Cystectomy	5 (10%)	6 (12%)	2 (9.53%)	2 (9.53%)
*RFS, median (range), month	11 (4, 22)	36 (24, 70)	18 (12, 23)	30 (24, 36)

*_**MIS**_ means muscle-invasive state, including two states, the NMIBC (Stage ≤ T1) and MIBC (Stage ≥ T2)

SLE means the submucosal linear enhancement of the tumor base on the DCE MR images

Tumor sizeindicates the largest tumor diameter in the lumen if multifocal tumor appeared, because the histo-pathological outcomes archived were based on the largest tumor site in the lumen in this circumstance

NoT is the abbreviation of “number of tumors” in the bladder lumen before operation.

RFSrepresents the recurrence-free survival time.

Table 2:

Results of the optimal radiomics features selected by using SVM-RFE and LASSO with a non-linear SVM classifier, respectively, for TFTY BCa recurrence prediction in both cohorts

Selection approach	Feature size	Cohort	*Sen	*Spe	*Acc	AUC	95% CI		*p*-value
							Lower	Upper	
SVM-RFE	32	Training	84.00%	80.00%	82.00%	0.8593	0.8425	0.8810	<< 0.01
		Validation	77.78%	73.83%	75.52%	0.8216	0.8130	0.8301	<< 0.01
LASSO	21	Training	73.74%	71.08%	72.41%	0.7504	0.7364	07613	< 0.05
		Validation	55.56%	75.00%	66.67%	0.7222	0.7003	0.7328	< 0.05

*Sen, Spe and Acc indicate average sensitivity, specificity and accuracy obtained by using the selected radiomics features and a non-linear SVM classifier.

Table 3:

Univariate and multivariate regression analyses of the indicators for recurrence prediction in the training cohort

Indicators	Univariate				Multivariate			
	#OR	95% CI		*p*-value	OR	95% CI		*p*-value
		Lower	Upper			Lower	Upper	
Age	1.602	0.759	3.380	0.206	—	—	—	—
Gender	1.569	0.239	1.876	0.22	—	—	—	—
Grade	1.195	0.370	3.858	0.09	—	—	—	—
MIS	**3.857**	**1.180**	**12.696**	**< 0.05**	**2.166**	**1.154**	**4.066**	**< 0.05**
Stalk	0.231	0.066	0.810	0.017	0.408	0.089	1.868	0.248
SLE	**0.457**	**0.197**	**1.063**	**< 0.05**	0.542	0.126	2.335	0.411
TumorSize	1.002	0.969	1.036	0.9	—	—	—	—
NoT	**1.534**	**1.176**	**2.564**	**< 0.05**	1.067	0.936	2.425	0.513
Operation	0.542	0.271	1.927	0.300	—	—	—	—
Rad-Score	**8.682**	**2.942**	**25.620**	**<< 0.05**	**8.191**	**2.415**	**27.780**	**<< 0.05**

Bold and **underlined** indicates statistical significance at the level of *p*-value <0.1.

#**OR** means odds ratio.

Table 4:

Performance of different models for patients' RFS estimation in the training cohort

Model for RFS estimation	Harrell's C-index	95% CI		*p*-value
		Lower	Upper	
Clinical model	0.689	0.589	0.792	< **0.05**
Radiomics model	0.832	0.761	0.895	< **0.05**
Radiomics and clinical model	0.897	0.812	0.926	< **0.05**